Supplementary Materials

Optical and Electrochemical Properties of Multi-layer Polyelectrolyte Thin Films Incorporating Spherical, Gold Colloid Nanomaterials

Tran T. Doan, Robert W. Day, Michael C. Leopold*

Department of Chemistry, Gottwald Center for the Sciences, University of Richmond Richmond, VA 23173

Contents:

* To whom correspondence should be addressed. Email: mleopold@richmond.edu. Phone: (804) 287-6329. Fax: (804) 287-1897.

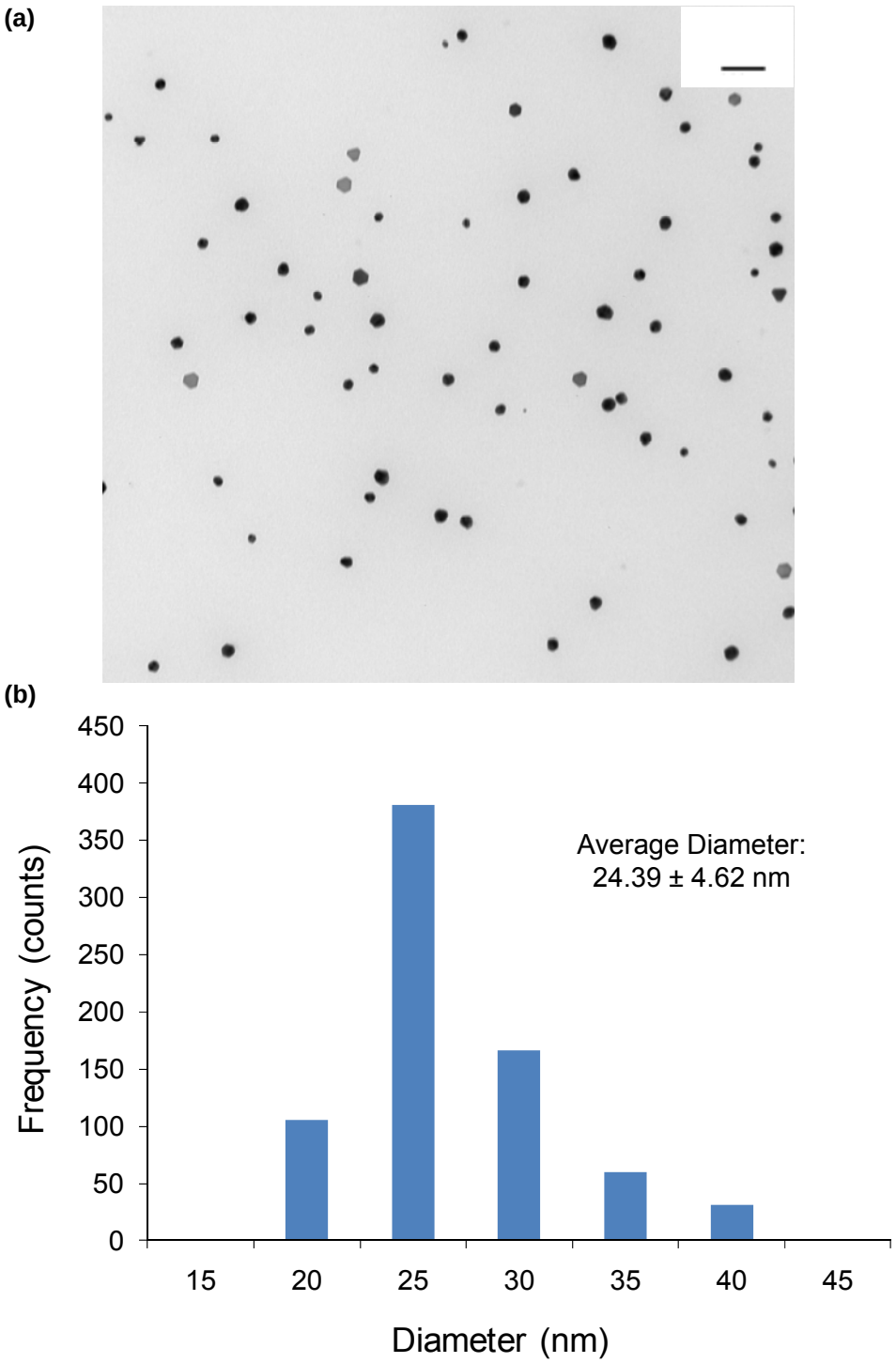

Fig. SM-1 (a) Typical transmission electron microscopy (TEM) image of aqueous Ag-NPs at 25000x magnification. The bar in the upper right corner signifies 100 nm. (b) Histogram analysis of core size determined from TEM imaging

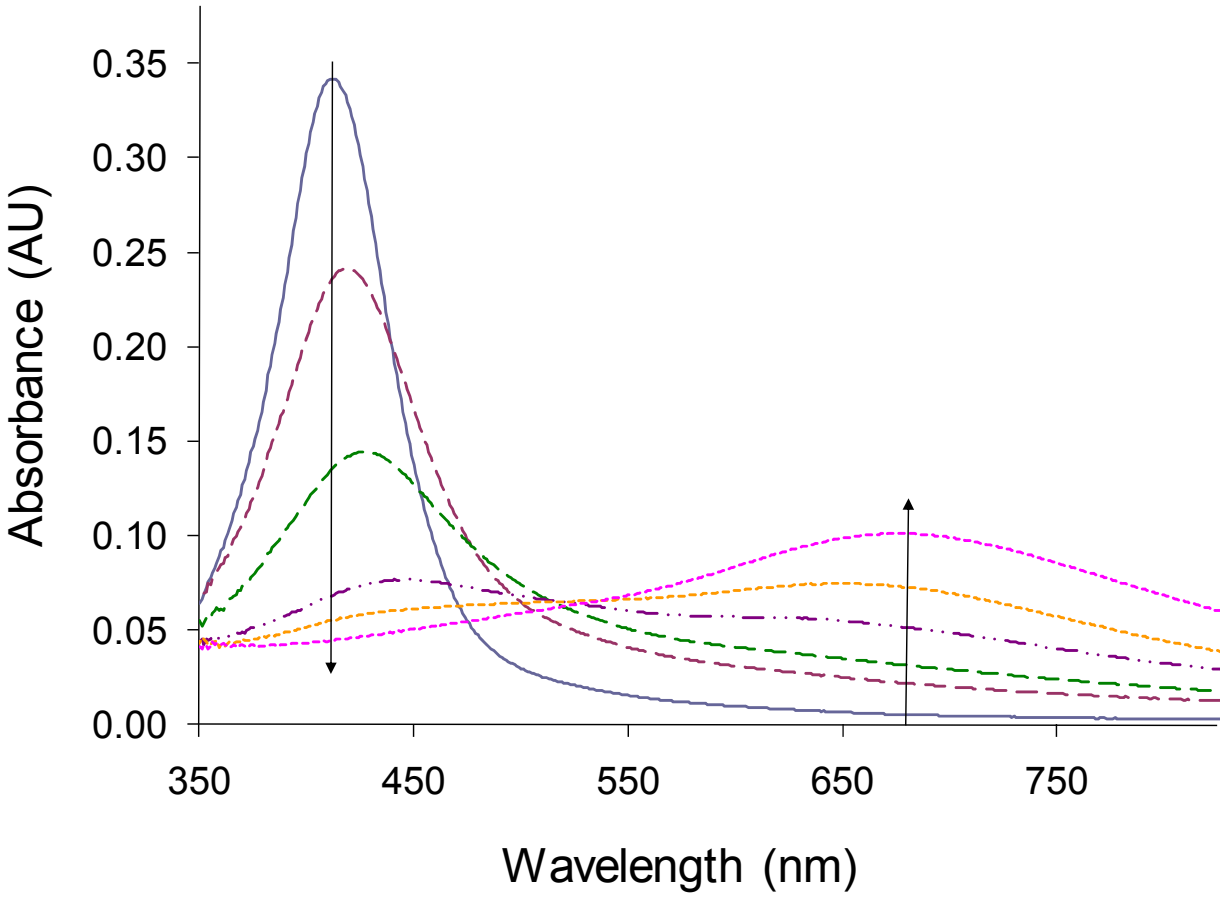

Fig. SM-2 The progression of hollow gold nanoshell synthesis reaction is spectrally tracked. Aliquots of 1 mM gold salt are added until the surface plasmon band (SPB) of the Ag-NPs at ~420 nm slowly dissipates and SPB of the Au nanoshells develops at ~680 nm

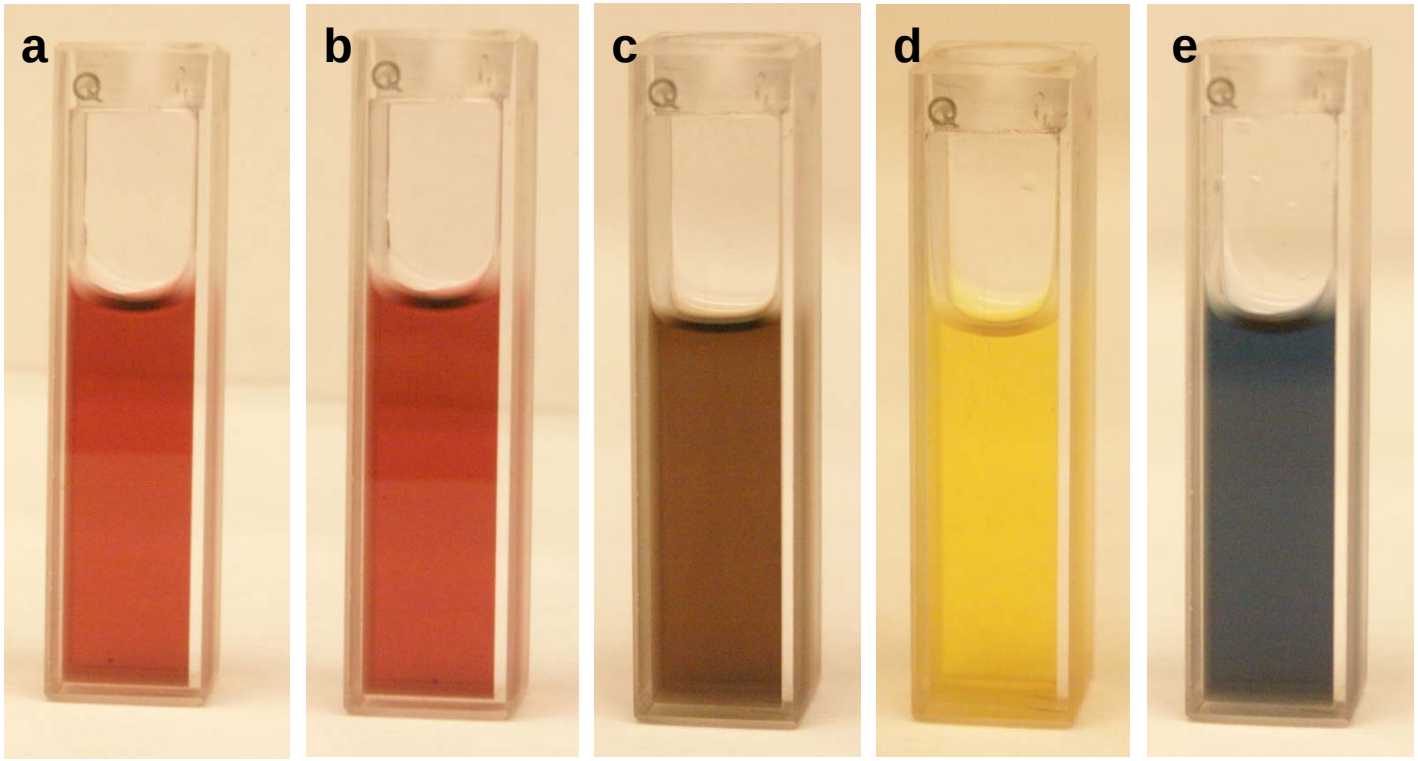

Fig. SM-3 Digital photographs of bulk solutions of the NMs embedded into the PEM films including: (a) CS-NPs (wine red); (b) TAS-NPs (wine red); (c) MUA-MPCs (brown); (d) Ag NP precursors; and (e) Au-NSs (blue). Note: Thin films with only one embedded layer of NMs are largely transparent with only a slight coloring that is nearly invisible to the naked eye

Table SM-1 Absorption spectra λ_{max} average shift comparison of NMs in bulk solution vs. immobilized within a film (zero layers of PE)

Nanomaterial	λ_{max} solution (nm)	λ_{max} film (nm)[†]	$\Delta\lambda_{max}$ (nm)
CS-NPs	520	525	5
TAS-NPs	520	525	5
Ag-NPs	410	N/A	N/A
Au-NSs	680	700	20
MUA-MPCs	N/A	N/A	N/A

[†] Measured at zero layers of PE adlayers.

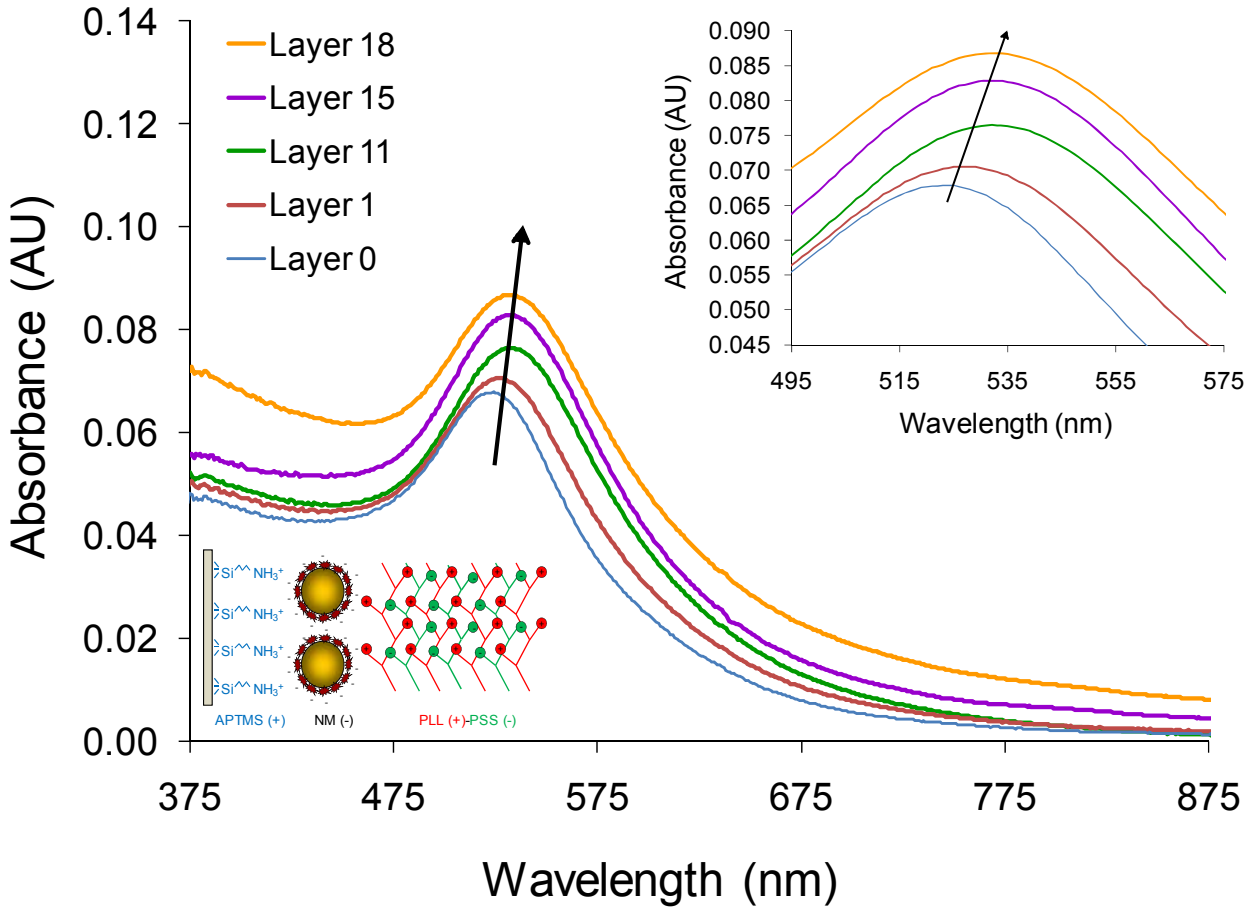

Fig. SM-4 Absorbance spectra of PE multilayered films built according to the Scheme I with embedded CS-NPs on 3-APTMS-modified slides and measured in NP H_2O. Insets display the smaller spectral window around λ_{max} of the surface plasmon band (SPB). Note: When incorporated into thin films, CS-NPs are prone to stability issues and often aggregate as indicated by a red shifted peak emerging as aggregation progresses.[1,23-27] Care should be used to minimize exposure of such films to ambient air and their use within films to be developed into potential sensors is not recommended if the other NMs (e.g., TAS-NPs) are available

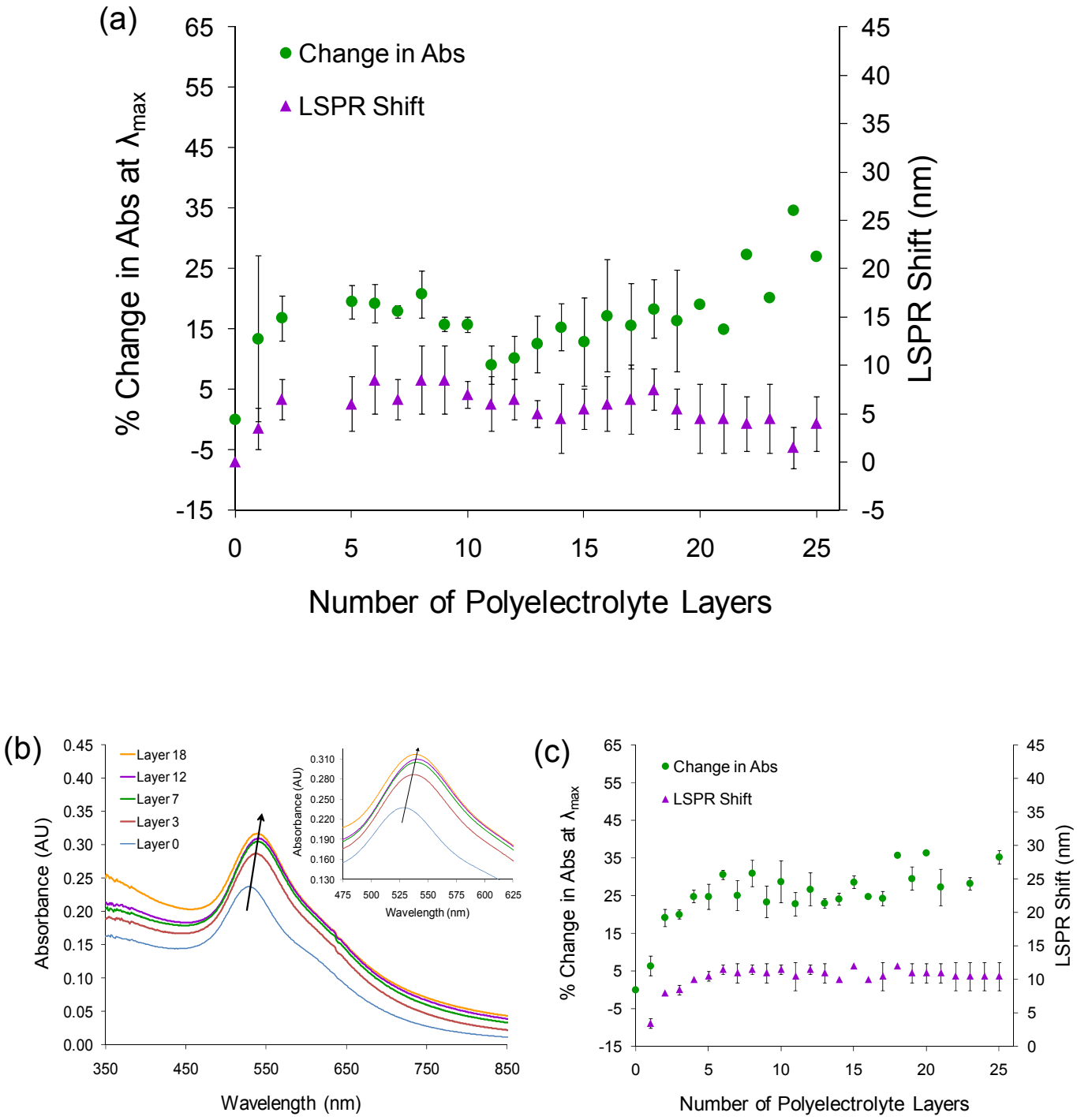

Fig. SM-5 (a) Tracking the percent change in absorbance at λ_{max} and the red shift of the localized surface plasmon resonance (LSPR) for films assembled via Scheme 1 on glass slides with CS-NPs. Note: In some cases, the error bars are smaller than the data markers. (b,c) The same results shown in SM-4 and SM-5a for a significantly thicker PEM embedded with more than a submonolayer of CS-NP that indicates the same trends

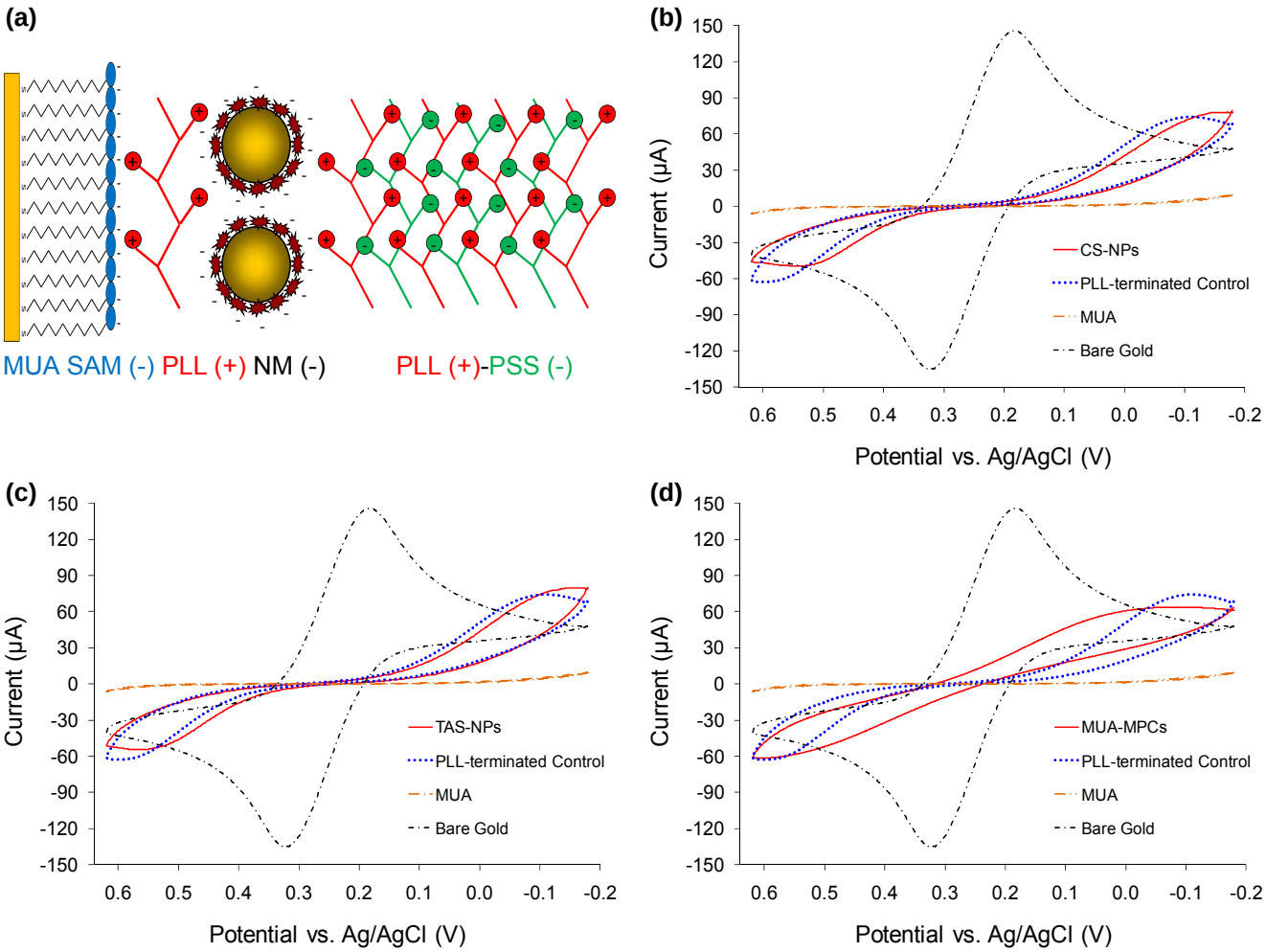

Fig. SM-6 (a) Schematic of a film constructed for electrochemical investigation adapted from Scheme I of a MUA SAM-modified gold electrode, a PLL anchoring PE layer, negatively charged NM, and 7 alternating PLL and PSS layers; Cyclic voltammetry (CV) of 5 mM ferricyanide in 0.5 M KCl supporting electrolyte at 100 mV/sec at bare gold, MUA SAM-modified gold, and PLL-terminated PEM films with and without (control) embedded (b) CS-NPs, (c) TAS-NPs, or (d) MUA-MPCs. CV results at films incorporating Au-NSs (Fig. 5b), CS-NPs, and TAS-NPs were similar while results at MUA-MPCs films expressed slightly more blocking behavior than the other NMs

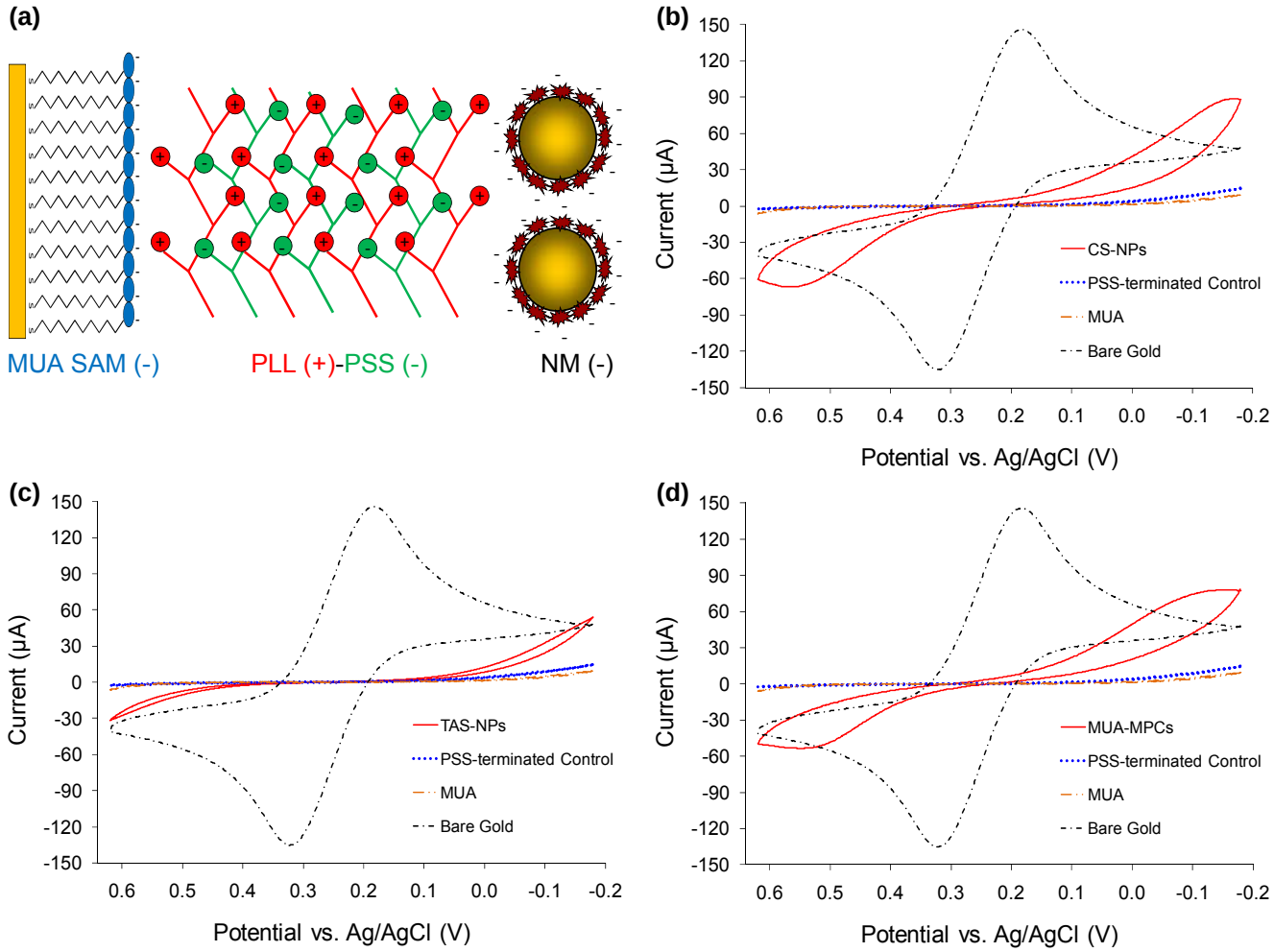

Fig. SM-7 (a) Schematic of a film constructed for electrochemical investigation adapted from Scheme II of a MUA SAM-modified gold electrode, 7 alternating PLL and PSS layers, and negatively charged NM. Cyclic voltammetry (CV) of 5 mM ferricyanide in 0.5 M KCl supporting electrolyte at 100 mV/sec at bare gold, MUA SAM-modified gold, and PSS-terminated PEM films with and without (control) embedded (b) CS-NPs, (c) TAS-NPs, or (d) MUA-MPCs. CV results at films incorporating Au-NSs (Fig. 6a), CS-NPs, and MUA-MPCs were similar while results at TAS-NPs films expressed slightly increased blocking behavior than the other NMs

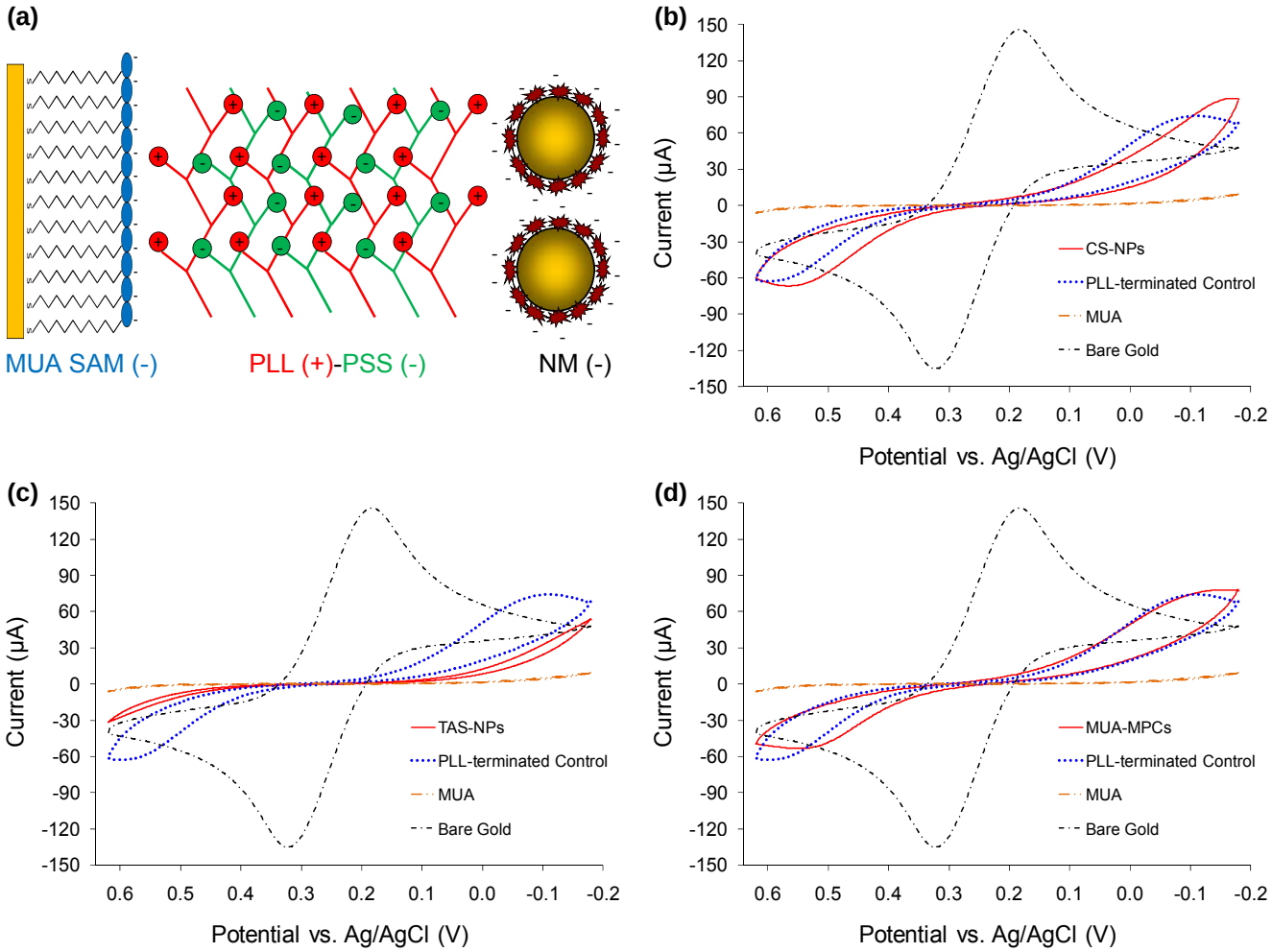

Fig. SM-8 (a) Schematic of a film constructed for electrochemical investigation adapted from Scheme II of a MUA SAM-modified gold electrode, 7 alternating PLL and PSS layers, and negatively charged NM. Cyclic voltammetry (CV) of 5 mM ferricyanide in 0.5 M KCl supporting electrolyte at 100 mV/sec at bare gold, MUA SAM-modified gold, and PLL-terminated PEM films with and without (control) embedded (b) CS-NPs, (c) TAS-NPs, or (d) MUA-MPCs. CV results at films incorporating Au-NSs (Fig. 6a), CS-NPs, and MUA-MPCs were similar while results at TAS-NPs films expressed slightly increased blocking behavior than the other NMs

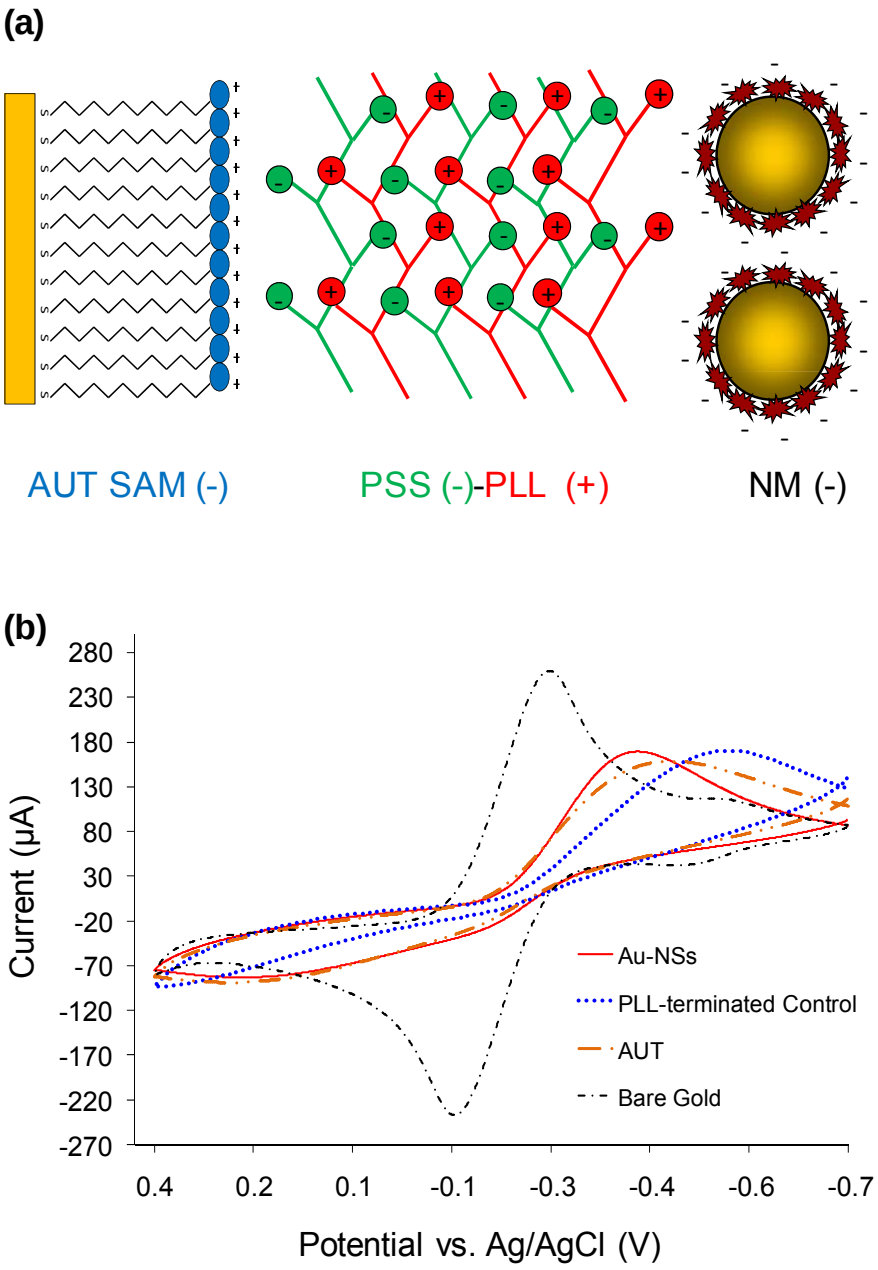

Fig. SM-9. (a) Schematic for alternative film assembly with opposite electrostatic interactions (using a base cationic SAM of 11-amino-1-undecanethiol as opposed to the anionic MUA SAM. (b) Cyclic voltammetry (CV) of 5 mM ruthenium hexamine in 0.5 M KCl supporting electrolyte at 100 mV/sec at bare gold, MUA SAM-modified gold, and PLL-terminated PEM film with and without (control) embedded Au-NSs